Issues of "Standard" Explosion Tests for non-spherical Dusts

Valeria Di Sarli[a,*], Enrico Danzi[b], Luca Marmo[b], Roberto Sanchirico[a], Almerinda Di Benedetto[c]

[a]Istituto di Ricerche sulla Combustione, Consiglio Nazionale delle Ricerche (CNR), Piazzale V. Tecchio 80, 80125, Napoli, Italy
[b]Dipartimento Scienza Applicata e Tecnologia, Politecnico di Torino, Corso Duca degli Abruzzi 24, 10129, Torino, Italy
[c]Dipartimento di Ingegneria Chimica, dei Materiali e della Produzione Industriale, Università degli Studi di Napoli Federico II, Piazzale V. Tecchio 80, 80125, Napoli, Italy
valeria.disarli@irc.cnr.it

Measurements of the flammability and explosion parameters for non-spherical dusts are performed according to standard procedures in standard explosion equipment developed and tested for spherical dusts.
Studies have shown that the standard procedures and equipment applied to spherical particles suffer from many issues: control of the turbulence level, non-uniform dust dispersion, and particle fragmentation due to the injection system. The applicability of the standard procedures and equipment to non-spherical particles is still an open issue.
In this work, we have investigated, via CFD simulations, the distribution of turbulence and dust concentration in the standard 20 l spherical vessel for non-spherical particles. Results have shown that a higher turbulence level and a higher amount of dust actually fed into the vessel are reached with respect to spherical particles.

1. Introduction

In many industrial applications, fiber-like dusts are used such as textile fibers, biomasses, fibrous wood and polyethylene dusts. In the last years, many accidents occurred as a consequence of fires and explosions involving biomass dusts (Butcher, 2011; Holland, 2011), wool dusts (Salatino et al., 2012), and polyethylene dusts (Amyotte et al., 2012; Di Benedetto et al., 2010). As a consequence, the evaluation of the flammability and explosion parameters for fiber-like dusts is a demanding step.

Measurements of the most important flammability and explosion parameters for dusts are performed according to standard procedures in a standard explosion apparatus consisting of a closed steel combustion chamber with an internal volume of 20 l, spherical or cylindrical in shape. One of the major requirements of the apparatus is that it must be capable of dispersing a fairly uniform dust cloud in the vessel and of realizing a controlled turbulence level.

Studies have shown that the standard procedure and equipment applied to spherical particles suffer from many issues. The first issue is the inability to control the turbulence level inside the sphere, which varies in time, space and with the properties of the dust (Dahoe et al., 2001; Di Benedetto et al., 2013; Hauert et al., 1994; Pu et al., 1990). Furthermore, it has been shown, via CFD simulations, that with the standard procedure/equipment it is not possible to generate a uniform dust-air cloud (Di Benedetto et al., 2013; 2015; Di Sarli et al., 2013; 2014; 2015; 2018). The third issue is that the method of dust injection into the sphere may cause severe particle fragmentation, thus changing the particle size distribution of the dust and altering its flammability and explosion features (Kalejaiye et al., 2010; Sanchirico et al., 2015).

The applicability of the standard procedures and equipment to non-spherical particles is still an open issue. Wilén et al. (1999) tested several fibrous biomass samples. They used different dispersion systems to obtain the same values of deflagration index, K_{St}, as the standard system. However, the reproducibility of other parameters has not been proven.

García-Torrent et al. (1998) and Conde Lázaro & García Torrent (2000) used extended 25 l dust holders for high dust loadings for hyperbaric explosion tests with biomass. They modified the ignition delay and the

dispersion pressure and, in turn, concluded that the results obtained were not comparable to the standard system due to varied turbulence levels.

Marmo et al. (2010; 2018) studied the explosibility of textile fibers in the 20 l sphere equipped with a rebound nozzle, showing that issues on dispersion and turbulence generation arise due to the non-spherical flocculent nature and the limited dustability of these materials.

Amyotte et al. (2012) investigated the explosion features of fibrous wood and polyethylene dusts of different particle sizes. At high concentrations and larger particle size, part of the dust was placed directly inside the 20 l sphere fitted with a rebound nozzle. This practice, also used by Iarossi et al. (2012; 2013) with polyamide and polyester fibers, was likely to result in variability of dust dispersion patterns, and the results showed that the maximum explosion pressure for wood samples was indeed variable.

Slatter et al. (2015) demonstrated that the explosion/flammability parameters of fibrous dusts are quite affected by the dispersion system.

In this work, we have investigated, via CFD simulations, the ability of the 20 l spherical explosion vessel of dispersing non-spherical particles with a controlled turbulence level.

2. The CFD Model

The model consists of the time-averaged Navier-Stokes equations. Turbulence was modelled by using the standard k-ε model (Launder and Spalding, 1972). Solid phase flow was solved by implementing the Lagrangian approach with the Discrete Phase Model (DPM). Accordingly to the classification by Elghobashi (1994), the two-way coupling was used to model the interaction between the fluid phase and the solid particles.

When simulating non-spherical particles, a shape factor (sf) was introduced. This factor is defined as the ratio between the surface area to the surface area of a spherical particle with the same equivalent diameter. The shape factor affects the drag force.

The fluid flow equations were discretized using a finite-volume formulation on a 3D non-uniform unstructured grid. The model equations were discretized by using first order schemes for convective terms and second order schemes for diffusion terms. First-order time integration was used to discretize temporal derivatives with a time step of $1 \cdot 10^{-4}$ s.

The DPM is described by ordinary differential equations. For particle tracking, we used an automated scheme which provides a mechanism to switch in an automated fashion between numerically stable lower order schemes and higher order schemes, which are stable only in a limited range. The Euler integration as lower order scheme and the semi-implicit trapezoidal integration as higher order scheme were used, with a particle tracking integration time step equal to $1 \cdot 10^{-4}$ s.

Parallel computations were performed by means of the segregated pressure-based solver of the code ANSYS Fluent (release 17.0) (www.ansys.com).

The simulation conditions are listed in Table 1.

Table 1: Simulation conditions

Volume of the dust container [l]	0.6
Volume of the sphere [l]	20
Initial pressure of the dust container [bar]	21
Initial pressure of the sphere [bar]	0.4
Dust density [kg/m^3]	2046
Dust diameter [μm]	250
Dust concentration [g/m^3]	250
Shape factor (sf) [-]	1; 2

3. Results

CFD simulations were performed by assuming size of the non-spherical particles equal to 250 μm and shape factor (sf) equal to 1 and 2. The results for the spherical particles (with diameter of 250 μm) were obtained in a previous work (Di Benedetto et al., 2013), and are here reported for the sake of comparison.

In Figure 1, the maps of the turbulence kinetic energy (TKE) are shown as computed for spherical and non-spherical dusts at 60 ms (ignition time).
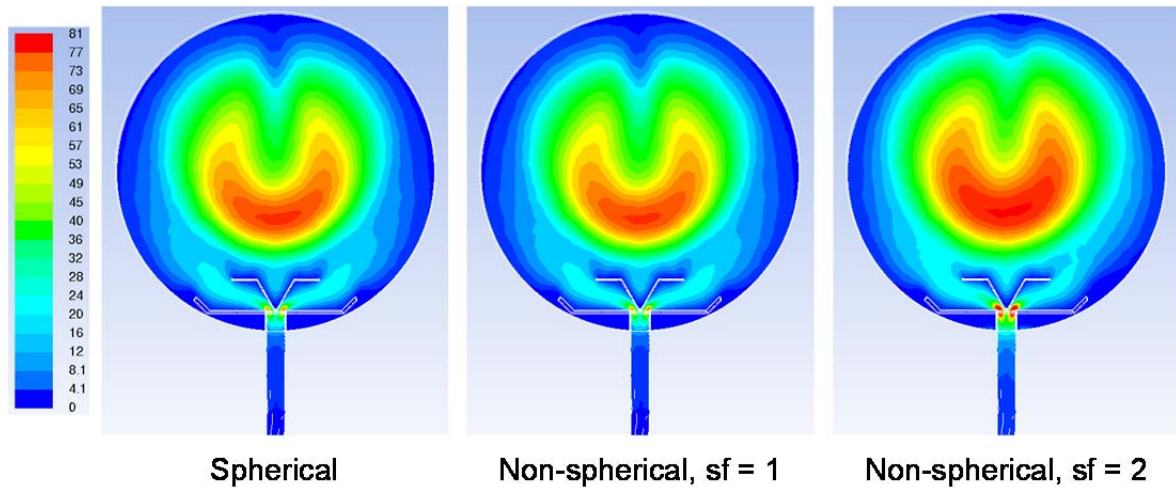
Figure 1: Maps of TKE [m²/s²] at t = 60 ms as computed for spherical dust and non-spherical dust with sf = 1 and 2.

In all cases, the TKE is strongly non-uniform inside the sphere.

Figure 2 shows the time histories of TKE as computed in the center of the sphere for the three cases. This figure allows quantification of the turbulence level in the zone where ignition takes place.
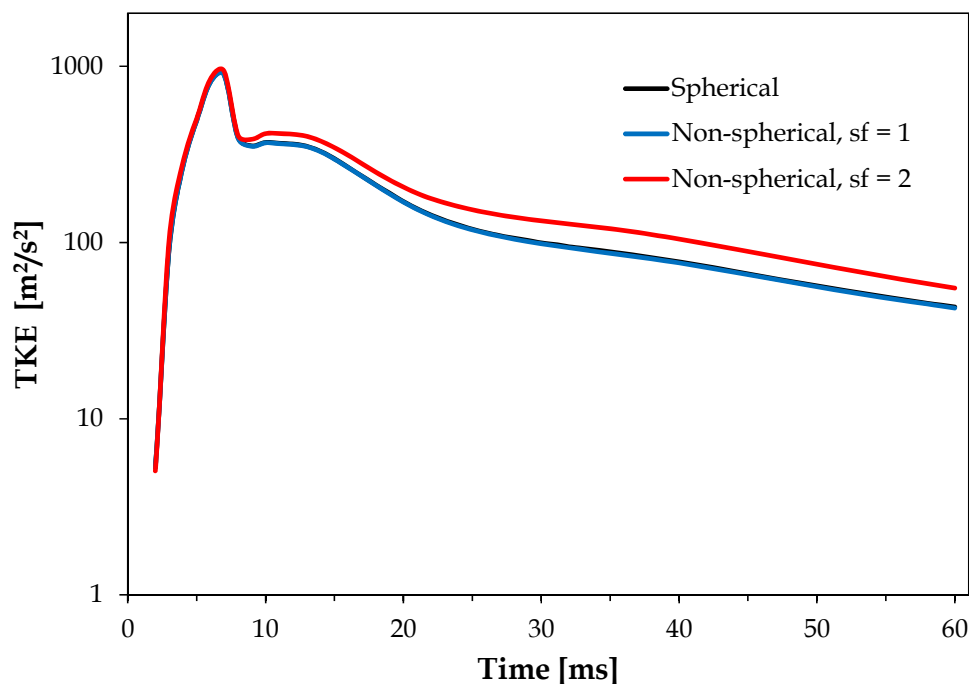

Figure 2: TKE [m²/s²] versus time as computed in the center of the vessel for spherical dust and non-spherical dust with sf = 1 and 2.

The three plots are nearly superimposable during both the phase of turbulence build-up and the initial phase of turbulence decay. However, the TKE attained at the ignition time (60 ms) in the case of non-spherical dust with sf = 2 (55 m²/s²) is higher than that attained in the cases of sf = 1 and spherical dust (43 m²/s²). This trend is in agreement with the results by Bellani et al. (2012) who investigated the impact of particle shape on turbulence. They found that spherical particles provide a 15 % TKE reduction relative to a flow without particles. This is a much larger impact than that shown by ellipsoidal particles, which cause a reduction of only

3 %. The reason for this lies in the details of the flow near the particle surface, which lead to changes in production and dissipation of TKE, as well as redistribution of TKE across scales.

In a previous work (Di Benedetto & Russo, 2007), we proposed a modification of the correlation by Dahoe et al. (1996) for the evaluation of the deflagration index, K_{St}, to take into account the effect of turbulence. In particular, we substituted the laminar burning velocity (S_l) with the turbulent burning velocity (S_t), which varies with the turbulence level (u'):

$$K_{St} = \left(\frac{dP}{dt}\right)_{max} V^{1/3} = \frac{3(P_{max} - P_o)}{R_{vessel}}\left(\frac{P_{max}}{P_o}\right)^{\frac{1}{\gamma}} S_t(u') \tag{1}$$

We tested several equations available in the literature for calculating S_t as a function of u', and the best agreement was obtained when using the correlation proposed by Pocheau (1994):

$$K_{St} = \left(\frac{dP}{dt}\right)_{max} V^{1/3} = \frac{3(P_{max} - P_o)}{R_{vessel}}\left(\frac{P_{max}}{P_o}\right)^{\frac{1}{\gamma}} S_l \sqrt{([1+(u'/S_l)^2])} \tag{2}$$

In order to quantify the effect of different turbulence levels on the violence of explosion, we used Eq. (2) to calculate K_{St} for spherical dust and non-spherical dust with sf = 1 and 2. Table 2 shows the results in terms of ratio β between K_{St} at a given sf and corresponding K_{St} for spherical particles.

Table 2: Values of u' and ratio β at sf = 1 and 2

sf [-]	u' [m/s]*	β [-]
1	5.3	1
2	6.1	1.14

*in the center of the sphere

The different turbulence level affects the values of K_{St}. In particular, in going from sf = 1 to sf = 2, the increase of u' leads to an increase of K_{St} of about 14 %.

In Figure 3, the particle tracks colored by the dimensionless dust concentration are shown as computed for spherical and non-spherical dusts at 60 ms (ignition time).
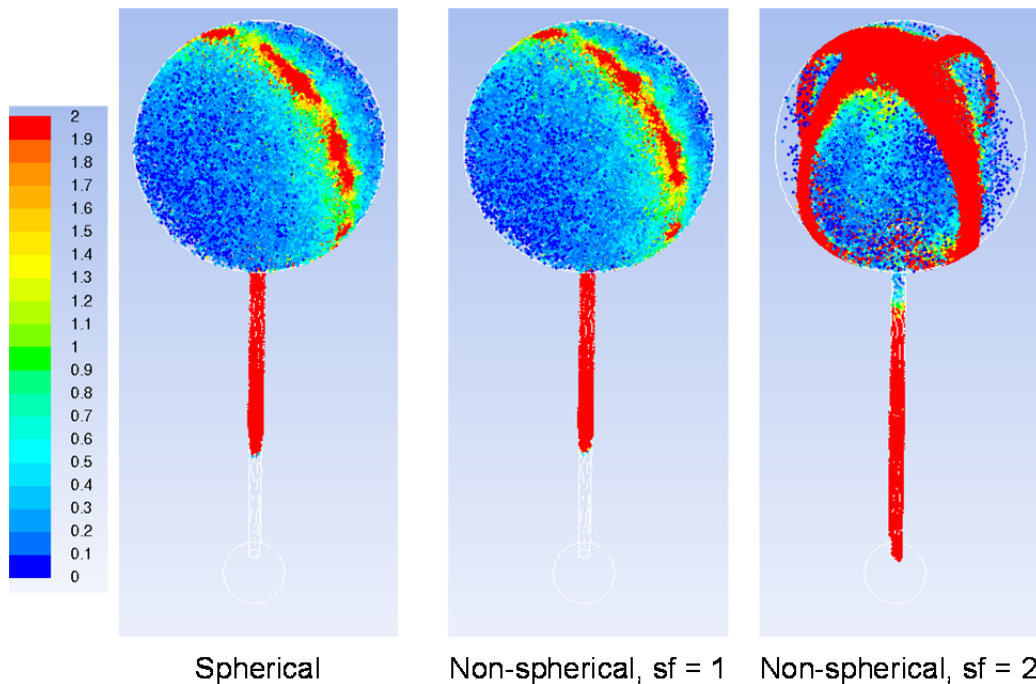

Spherical   Non-spherical, sf = 1   Non-spherical, sf = 2

Figure 3: Particle tracks colored by the dimensionless dust concentration at t = 60 ms as computed for spherical dust and non-spherical dust with sf = 1 and 2.

In all cases, the dust distribution is quite non-uniform. The main difference is in the amount of dust actually fed into the sphere. In the case of non-spherical particles with sf = 2, this amount is around 10 % higher than in the cases of spherical particles and non-spherical particles with sf = 1.

Overall these results suggest that measurements of K_{St} may be significantly affected by the shape of dust particles, not only due to chemical and physical issues but also due to test conditions.

4. Conclusions

The shape of the dust particles significantly affects the spatial distribution of turbulence and dust concentration inside the explosion vessel. In particular, at the ignition time (60 ms), the turbulence kinetic energy at the center of the sphere, where ignition is provided, is higher in the case of non-spherical dusts than in the case of spherical dusts. These results suggest that also the flame propagation and, consequently, the deflagration index will be different. Thus, novel standard procedures and equipment have to be developed in order to measure repeatable and reliable values of explosion and flammability parameters, which are dependent only on chemical and physical phenomena, and are completely unaffected by test conditions.

References

Amyotte P.R., Cloney C.T., Khan F.I., Ripley R.C., 2012, Dust explosion risk moderation for flocculent dusts, Journal of Loss Prevention in the Process Industries, 25, 862–869.

Bellani G., Byron M.L., Collignon A.G., Meyer C.R., Variano E.A., 2012, Shape effects on turbulent modulation by large nearly neutrally buoyant particles, Journal of Fluid Mechanics, 712, 41–60.

Butcher J., 2011, Firefighters battle huge biomass fire at Port of Tyne <http://www.journallive.co.uk/north-east-news/todaysnews/2011/10/31/firefighters-battle-huge-biomass-fire-at-port-of-tyne-61634-29689277/> accessed 13.10.2018.

Conde Lázaro E., García Torrent J., 2000, Experimental research on explosibility at high initial pressures of combustible dusts, Journal of Loss Prevention in the Process Industries, 13, 221–228.

Dahoe A.E., Cant R.S., Scarlett B., 2001, On the decay of turbulence in the 20-liter explosion sphere, Flow, Turbulence and Combustion, 67, 159–184.

Dahoe A.E., Zevenbergen J.F., Lemkowitz S.M., Scarlett B., 1996, Dust explosions in spherical vessels: The role of flame thickness in the validity of the 'cube-root law', Journal of Loss Prevention in the Process Industries, 9, 33–44.

Di Benedetto A., Di Sarli V., Russo P., 2010, On the determination of the minimum ignition temperature for dust/air mixtures, Chemical Engineering Transactions, 19, 189–194.

Di Benedetto A., Russo P., 2007, Model for the evaluation of thermo-kinetic parameters of dust explosions, IChemE Symposium Series, 153, 123/1–123/5.

Di Benedetto A., Russo P., Sanchirico R., Di Sarli V., 2013, CFD simulations of turbulent fluid flow and dust dispersion in the 20 liter explosion vessel, AIChE Journal, 59, 2485–2496.

Di Benedetto A., Russo P., Sanchirico R., Di Sarli V., 2015, A fan-equipped reactor for dust explosion tests, AIChE Journal, 61, 1572–1580.

Di Sarli V., Russo P., Sanchirico R., Di Benedetto A., 2013, CFD simulations of the effect of dust diameter on the dispersion in the 20 l bomb, Chemical Engineering Transactions, 31, 727–732.

Di Sarli V., Russo P., Sanchirico R., Di Benedetto A., 2014, CFD simulations of dust dispersion in the 20 L vessel: Effect of nominal dust concentration, Journal of Loss Prevention in the Process Industries, 27, 8–12.

Di Sarli V., Sanchirico R., Di Benedetto A., 2018, On the effect of initial pressure on the minimum explosive concentration of dust in air, Powder Technology, 336, 567–572.

Di Sarli V., Sanchirico R., Russo P., Di Benedetto A., 2015, CFD modeling and simulation of turbulent fluid flow and dust dispersion in the 20-L explosion vessel equipped with the perforated annular nozzle, Journal of Loss Prevention in the Process Industries, 38, 204–213.

Elghobashi S., 1994, On predicting particle-laden turbulent flows, Applied Scientific Research, 52, 309–329.

García-Torrent J., Conde-Lázaro E., Wilén C., Rautalin A., 1998, Biomass dust explosibility at elevated initial pressures, Fuel, 77, 1093–1097.

Hauert F., Vogl A., Radant S., 1994, Measurement of turbulence and dust concentration in silos and vessels, Proceedings of the 6th International Colloquium on Dust Explosions, Shenyang, PRC.

696

Holland T., 2011, Essex fire destroys 21000 tonnes of woodchip destined for Dalkia biomass plant <http://www.mrw.co.uk/news/essex-fire-destroys21000-tonnes-of-woodchip-destined-for-dalkia-biomass-plant/8617227.article/> accessed 13.10.2018.

Iarossi I., Amyotte P.R., Khan F.I., Marmo L., Dastidar A.G., Eckhoff R.K., 2012, Explosibility of polyamide and polyester fibers, Proceedings of Ninth International Symposium on Hazards, Prevention, and Mitigation of Industrial Explosions (July 22-27, 2012).

Iarossi I., Amyotte P.R., Khan F.I., Marmo L., Dastidar A.G., Eckhoff R.K., 2013, Explosibility of polyamide and polyester fibers, Journal of Loss Prevention in the Process Industries, 26, 1627–1633.

Kalejaiye O., Amyotte P.R., Pegg M.J., Cashdollar K.L., 2010, Effectiveness of dust dispersion in the 20-L Siwek chamber, Journal of Loss Prevention in the Process Industries, 23, 46–59.

Launder B.E., Spalding D.B., 1972, Lectures in Mathematical Models of Turbulence, Academic Press, London, England.

Marmo L., 2010, Case study of a nylon fibre explosion: An example of explosion risk in a textile plant, Journal of Loss Prevention in the Process Industries, 23, 106–111.

Marmo L., Sanchirico R., Di Benedetto A., Di Sarli V., Riccio D., Danzi E., 2018, Study of the explosible properties of textile dusts, Journal of Loss Prevention in the Process Industries, 54, 110–122.

Pocheau A., 1994, Scale invariance in turbulent front propagation, Physical Review E, 49, 1109–1122.

Pu Y.K., Jarosinski J., Johnson V.G., Kauffman C.W., 1990, Turbulence effects on dust explosions in the 20-liter spherical vessel, Symposium (International) on Combustion, 23, 843–849.

Salatino P., Di Benedetto A., Chirone R., Salzano E., Sanchirico R., 2012, Analysis of an explosion in a wool-processing plant, Industrial & Engineering Chemistry Research, 51, 7713–7718.

Sanchirico R., Di Sarli V., Russo P., Di Benedetto A., 2015, Effect of the nozzle type on the integrity of dust particles in standard explosion tests, Powder Technology, 279, 203–208.

Slatter D.J.F., Sattar H., Huéscar Medina C., Andrews G.E., Phylaktou H.N., Gibbs B.M., 2015, Biomass explosion testing: Accounting for the post-test residue and implications on the results, Journal of Loss Prevention in the Process Industries, 36, 318–325.

Wilén C., Moilanen A., Rautalin A., Torrent J., Conde E., Lödel R., Carlson D., Timmers P., Brehm K., 1999, Safe Handling of Renewable Fuels and Fuel Mixtures, VTT Technical Research Centre of Finland, Espoo 1999 (VTT PUBLICATIONS 394).